J. Phys. B: Atom. Molec. Phys. **13** (1980) 4849–4863. Printed in Great Britain

Scattering of intermediate-energy electrons by potassium†

L Vušković‡ and S K Srivastava

Jet Propulsion Laboratory, California Institute of Technology, Pasadena, California 91103, USA

Received 14 August 1979, in final form 4 June 1980

Abstract. Utilising a crossed electron-beam–atom-beam collision technique electron impact differential cross sections at 7, 20, 40, 60 and 100 eV incident energies have been determined for elastic scattering and for the following transitions from the ground state (4^2S) to (*a*) 4^2P, (*b*) 5^2S+3^2D, (*c*) 5^2P, (*d*) $4^2D+6^2S+4^2F+6^2P$ and (*e*) $5^2D+7^2S+5^2F$ states in potassium. Measurements were done in the scattering angular range of 5 to 120°. Values at angles smaller than 5° and larger than 120° have been obtained from extrapolation and the integral and momentum transfer cross sections have been calculated. Results are compared with available experimental and some selected theoretical data.

1. Introduction

Potassium is one of the species which recently has been identified in the Jovian environment (Vogt *et al* 1979). The radiation from these species has been observed by Voyager. The excitation mechanism for these emissions is believed to be via electron impact. The interpretation of the intense optical radiation requires laboratory data on electron impact excitation cross sections. This was the basic reason for carrying out the present experiments. At the same time, cross section data are also important for testing theoretical calculations which can be extended to energy regions where experimental measurements are not feasible.

The review paper of Bransden and McDowell (1978) has summarised all presently available experimental and theoretical results for electron scattering by potassium atoms at intermediate energies. Previous experimental data for electron scattering on potassium atoms include: (*a*) relative angular distributions for elastic scattering by McMillan (1934) and Gehenn and Wilmers (1971), (*b*) cross sections for elastic scattering and excitation of the (4^2P) and (5^2S+3^2D) by Williams and Trajmar (1977), (*c*) elastic and inelastic electron scattering by Buckman *et al* (1979), (*d*) excitation measurements of the resonance transition by Zapesochnyi *et al* (1976) and Chen and Gallagher (1978), (*e*) ionisation cross sections by McFarland and Kinney (1965) and Korchevoi and Przonski (1967) and (*f*) total cross sections by Kasden *et al* (1973). The theoretical work includes: (*a*) the Born approximation by Moiseiwitsch and Smith (1968), (*b*) the static model by Fink and Yates (1970), (*c*) the Glauber approximation by

† Work supported in part by National Aeronautics and Space Administration under Contract No NAS7-100 to the Jet Propulsion Laboratory and partially by the California Institute of Technology through the Caltech President's Fund.

‡ NRC/NASA Senior Resident Research Associate. Permanent address: Institute of Physics, PO Box 57, 11001 Belgrade, Yugoslavia.

0022-3700/80/244849+15$01.50

Walters (1976, 1973), (*d*) the optical model by Buckman *et al* (1979) and (*e*) the distorted-wave polarised orbital (DWPO) method by Kennedy *et al* (1977).

We have investigated elastic and inelastic processes almost up to the ionisation limit of potassium at electron impact energies of 7, 20, 40, 60 and 100 eV. The angular range covered is from 5 to 120°. Only two electronic transitions were resolved in the present experiments. Therefore, cross sections are presented for elastic scattering and for the following transitions to excited states from the ground (4^2S) states: 4^2P, 5^2S+3^2D, 5^2P, $4^2D+6^2S+4^2F+6^2P$ and $5^2D+7^2S+5^2F$. The differential cross sections in the angular regions between 0 and 5° and between 120 and 180° were obtained by extrapolation. These were then used in calculating the integral and momentum transfer cross sections.

The previous measurements of Williams and Trajmar (1977), which were performed in this laboratory, reported cross sections for several of the features presented in this paper. However, recent improvements in experimental procedures and data evaluation (§ 2) prompted a re-investigation of this atom over a wider range of both impact energy and energy loss. Where possible both the earlier data of Williams and Trajmar and the recent results of Buckman *et al* (1979) are compared with the present DCS.

2. Experimental techniques and procedures

The electron impact spectrometer used in the present study has been described in detail elsewhere (Trajmar *et al* 1977). Briefly, the apparatus consists of an electron gun, a hemispherical energy selector and analyser, electrostatic tube lenses, a spiraltron electron detector and the source for the potassium beam. The electron multiplier pulses are amplified and collected by a multichannel analyser. Data were processed by a microprocessor based computer and were stored on magnetic tapes for subsequent analysis.

The potassium beam is produced by resistive heating of a stainless steel crucible. The crucible has an exit channel of 0·1 cm inner diameter and 0·7 cm length. Upon heating, metal atoms effuse through this channel in the form of a collimated beam. On the side of the crucible was a 0·4 cm diameter hole which would be closed after filling the crucible with potassium. The potassium used was reagent grade 'Baker chemical' and was stored as small pieces in oil.

A coaxial resistive wire was wrapped around the crucible and heated it to a temperature sufficient to observe electron scattering. The crucible heating was monitored by a thermocouple gauge and the optimum operating conditions were established at a nominal temperature of 340 °C. No variation in the crucible temperature was observed during the acquisition of a complete data set. The variation in crucible temperature between each data set was observed to be less than 0·5% (338 to 342 °C). This variation produced a negligible effect on the geometrical correction applied to each data set. The crucible was covered with a mu-metal magnetic shield and a stainless steel assembly which was cooled by circulating chilled water. In the beginning of the experiment, the oven was gradually heated for about two to four hours in order to bake out the absorbed oil and other volatile impurities. At the same time the background pressure in the vacuum chamber was monitored. It increased when the temperature of the crucible rose. However, after all the oil and impurities evaporated the pressure in the chamber returned to the background value observed before heating began (2×10^{-7} Torr). By the end of this initial heating period the temperature of the crucible

reached a steady state and no subsequent fluctuation in the temperature or the heating current was observed during the entire experiment.

This method of heating had certain advantages. First of all, the temperature of the crucible could be controlled very accurately so that it could be operated at the lowest possible temperature to get measurable electron scattering from the potassium beam. For example, in the present experiment the crucible was heated to a temperature of about 340 °C which generated a vapour pressure of potassium of about 1 Torr within the crucible. At this pressure the potassium beam could be described by effusive flow conditions and was well defined. Secondly, because of the high heat capacity of the present heating system small fluctuations of temperature were eliminated. These fluctuations are difficult to control in the electron-bombardment heating technique for this low-temperature range (Williams and Trajmar 1977). Small fluctuations of temperature could cause large variations in the density of potassium atoms in the beam. For example, a 6% variation in the temperature of the crucible can cause a 60% variation in the density of atoms in the beam at about 340 °C. Therefore, these fluctitions can affect the intensity of scattered electrons drastically.

At sufficiently high crucible temperatures, scattering from the potassium dimer as well as double scattering from the strong resonant transition $4^2S \rightarrow 4^2P$ of potassium was observed. Since the double scattering occurs at a lower crucible temperature than potassium dimer formation, the energy-loss spectrum was monitored to determine the heating current at which double scattering was no longer observed. The crucible temperature during these experiments was kept below this value which was about 340 °C.

The primary electron beam was continuously monitored by a Faraday cup and was found to be very stable. The maximum change in the current during the measurement of one complete set of data was less than 3%. The incident energy of the primary beam was calibrated by measuring the position of the 19·36 eV resonance in He. For this purpose, the scattering chamber was filled with He and the elastic scattering intensity was monitored at 90° with respect to the primary beam as a function of incident energy. It was found that the contact potential was less than 0·5 eV. We estimate that the incident energies reported in this paper are accurate to within 0·5 eV. The true zero angle was measured by observing the nominal angle about which the intensity of the 4^2P transition of potassium was symmetric. The scattering angles are estimated to be accurate within 0·5°.

The data were taken between 5 and 120° scattering angles at impact energies of 7, 20, 40, 60 and 100 eV. It was found that the primary beam influenced the 5° elastic scattering at 7 and 20 eV impact energies. Since we were not able to determine the exact contribution of the primary beam, at these two energies we have not presented 5° data at 7 and 20 eV in this paper. The inelastic features for 100 eV impact energy were too weak at high scattering angles so we were not able to measure them accurately. Therefore, we present DCS values only up to 50° scattering angle for inelastic features at the impact energy of 100 eV.

Typical values for the energy resolution of the spectrometer during these measurements were 60 to 80 meV (FWHM). Due to this reason we could not resolve all the excited states of potassium. Typical energy-loss spectra of potassium are shown in figure 1.

For each impact energy, energy-loss spectra were obtained for 0 to 4·5 eV energy loss. These spectra were measured several times at each angle reported in the tables. From these spectra, at each impact energy, ratios of all the inelastic features with

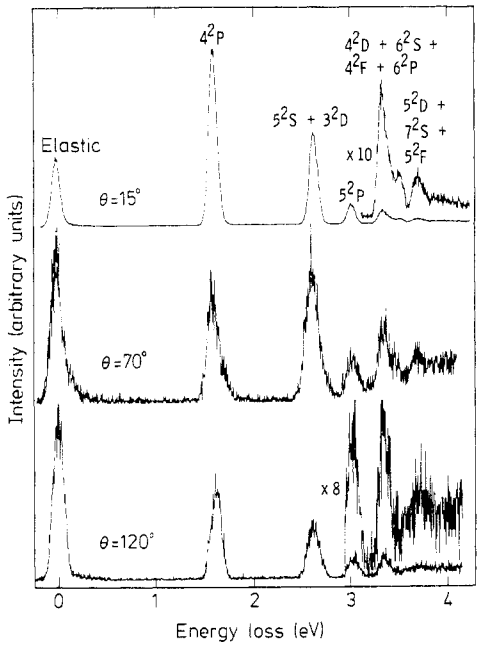

Figure 1. Electron impact spectra of potassium at 20 eV impact energy and at scattering angles θ as shown.

respect to the elastic feature were determined. The mean values obtained from these measurements were generally estimated to be accurate to within 10% at each angle and energy. Since the fourth ($4^2D+6^2S+4^2F+6^2P$) and fifth ($5^2D+7^2S+5^2F$) inelastic features (see figure 1) are weak, these ratios are more uncertain and are estimated to be accurate to within 30%.

Because the normalisation procedure used here (§§ 3.1 and 3.2) is very sensitive to the shape of the DCS angular distribution, particularly at low angles, special precautions were taken to determine these distributions accurately for both the elastic and resonance ($4^2S \rightarrow 4^2P$) transition. At each impact energy the angular distribution of the intensity for the elastic scattering and for the resonance transition was measured three to five times. These measurements agreed with each other within 5%. The resonance transition to elastic intensity ratios determined from these intensities agreed with the same ratios obtained from the energy-loss spectra to within 10%. Finally, the recent calculations of Trajmar and Brinkman (1980) were used to correct the resulting angular distributions for the effects of target geometry. This calculation takes into account the shape of the incident beam (which is different at low and high E_0), the shape of the target beam (which is proportional to the vapour pressure), as well as the slope of the relative DCS curve for a particular impact energy. The uncertainty in this geometrical factor is about 5% and a more detailed discussion of these effects may be found elsewhere (Vušković *et al* 1981).

As previously mentioned, the background pressure was about 2×10^{-7} Torr. Scattering from the background gases was an order of magnitude smaller than elastic scattering at the minimum of the DCS curve. Therefore the influence of background scattering was neglected. In addition to these precautions, care was taken in determining the relative intensity of each feature in the spectra. Instead of relying on peak intensity values (Williams and Trajmar 1977), the total counts in each feature were measured. This value was corrected for the background counts by first determining the

average background counts per channel in a transition-free region of the spectrum and then multiplying this by the number of channels included in the feature utilising a microprocessor based computer.

3. Results

3.1. Differential cross sections

Following the procedure described in § 2, we have obtained the elastic and all the inelastic cross sections for potassium in the same arbitrary units at each impact energy. The major problem is the transformation of any one of these relative cross sections to an absolute cross section. All the other transitions can then be put on the absolute scale since the intensity ratios between these transitions are known. There is, as yet, no satisfactory experimental method for determining the absolute values of metal vapour cross sections and present theoretical calculations are not reliable enough for normalisation of the experimental data for low-energy electron scattering. Therefore, we have decided to normalise the present data by using the generalised oscillator strength for an electron impact excitation process which has been defined (Inokuti 1971) by:

$$f^{G}(K) = \tfrac{1}{2} W(k_i/k_f) K^2 \mathrm{DCS}^{B}(K) \tag{1}$$

where W is the excitation energy, k_i and k_f are the magnitudes of the momentum of the electron before and after the collision respectively, K is the magnitude of the momentum transfer and $\mathrm{DCS}^{B}(K)$ is the Born cross section. It was shown by Bethe (1930) that in the limit $K \to 0$ the $f^{G}(K) \to f^{opt}$, where f^{opt} is the optical oscillator strength of a dipole, allowed transition. Lassettre *et al* (1969) further investigated the properties of equation (1) and found that $\mathrm{DCS}^{B}(K)$ can be replaced by an experimentally measured DCS which may not be given by the Born approximation. For such a case, $f^{G}(K)$ can be called an 'apparent generalised oscillator strength', $f_a^{G}(K)$, and it was shown that $f_a^{G}(K) \to f^{opt}$ in the limit $K \to 0$.

We have employed the f^{opt} value of the resonance transition, $4^2S \to 4^2P$ for the purpose of normalising the relative values of the DCS for this transition. The most accurate value of f^{opt} has been recommended by Dalgarno and Davison (1967) and is equal to $1{\cdot}01 \pm 5\%$.

The relative values for the DCS for the resonance transition were substituted in equation (1) in place of $\mathrm{DCS}^{B}(K)$ and the relative values of $f_a^{G}(K)$ were calculated for each scattering angle. The corresponding values of K were obtained from the following relation:

$$K^2 = k_i^2 + k_f^2 - 2k_i k_f \cos\theta. \tag{2}$$

Since the limit theorem of Lassettre *et al* (1969) enables one to extrapolate the $f_a^{G}(K)$ to $K^2 \to 0$ to obtain f^{opt}, regardless of the validity of the Born approximation (Inokuti 1971), the question that remained was how to approach the point $K^2 \to 0$. The lowest values of K^2, where present measurements have been done, are 0·011 and 0·056 au, for a 5° scattering angle at 7 and 100 eV incident energy, respectively.

It can be demonstrated through many examples (He, Hg, CO and H_2O, Lassettre *et al* 1970, Lassettre and Dillon 1973, Skerbele and Lassettre 1973, Lassettre and Skerbele 1974, Dillon and Lassettre 1975) that a plot of $\ln f_a^{G}(K)$ versus K^2 is close to a straight line for optically allowed transitions in the angular range below about 10°. On

this plot extrapolation to $K^2 = 0$ is especially easy. Atomic hydrogen serves as a useful guide for this problem since it is the simplest atom with a single valence electron and is theoretically well understood (Inokuti 1971). Born calculations indicate that $\ln f^G(K)$ for the $1s \rightarrow 2p$ excitation in atomic hydrogen exhibits a nearly perfect linear dependence on K^2 for $0 \leq K^2 \leq 0{\cdot}86$ corresponding to a 20° scattering angle at 100 eV impact energy. We owe this observation to M Inokuti and M Dillon (personal conversation). For systems other than hydrogen, the Lassettre (1965) power series can be applied. Therefore, the argument probably holds the same way. This justification for the linear dependence of $\ln f^G(K)$ as a function of K^2 is valid only within the Born approximation. Recent experimental investigation on the resonance transition in lithium (Vušković *et al* 1981) shows that a linear dependence can also be applied at low impact energies. Additional justification for the present normalisation procedure comes from the good agreement of the present integral cross sections with the measurements of Chen and Gallagher (1978).

Since the present measurements extend down to 5° scattering angle, $\ln f_a^G(K)$ was numerically extrapolated to $K^2 = 0$ assuming the straight-line dependence. At $K^2 = 0$, $f_a^G(K)$ equals f^{opt}. This procedure was used at each electron impact energy and absolute values of the DCS were obtained by using $1{\cdot}01 \pm 0{\cdot}05$ for the optical oscillator strength.

The differential cross sections for elastic scattering and for the excitation of 4^2P, $5^2S + 3^2D$, 5^2P, $4^2D + 6^2S + 4^2F + 6^2P$ and $5^2D + 7^2S + 5^2F$ states are listed in tables 1, 2, 3, 4 and 5 for impact energies of 7, 20, 40, 60 and 100 eV respectively. The error associated with the DCS is approximately 18% and is calculated as the square root of the sum of the squares of the contributing errors. These errors arise from three principal sources: the relative shape of the DCS, the geometrical correction and the normalisation procedure. The relative DCS is estimated to be accurate to about 10%. Uncertainties in the shape arise from drift in the primary beam (about 3%) and the scattering angle (about 0·5°) as well as from the statistics associated with the number of counts recorded for each energy-loss feature. For the feature represented by the last two columns in tables 1–5, the statistical uncertainties are by far the largest and increase the estimated errors in the DCS to about 35%. The error in the geometrical correction arises from

Table 1. Differential cross sections (in units $10^{-20}\,m^2\,sr^{-1}$) for electron scattering by potassium at 7 eV impact energy.

θ (deg)	Elastic	4^2P	$5^2S + 3^2D$	5^2P	$4^2D + 6^2S + 4^2F + 6^2P$	$5^2D + 7^2S + 5^2F$
5	—	474·0	51·4	2·45	17·0	0·863
10	97·1	160·0	27·9	2·76	3·85	1·08
15	50·2	63·9	16·6	1·90	2·76	0·790
20	18·9	21·0	9·08	0·972	2·31	0·596
30	5·38	2·92	2·55	0·212	0·648	0·280
40	3·06	1·11	0·861	0·0728	0·272	0·126
50	1·78	0·598	0·328	0·0400	0·0909	0·0358
60	1·13	0·372	0·223	0·0405	0·0682	0·0279
70	0·664	0·260	0·104	0·0286	0·0282	0·0204
80	0·764	0·201	0·0957	0·0162	0·0313	0·0203
90	1·08	0·218	0·100	0·0207	0·0253	0·0319
100	1·17	0·285	0·172	0·0372	0·0494	0·0647
110	0·903	0·260	0·163	0·0410	0·0436	0·0735
120	0·424	0·176	0·143	0·0408	0·0394	0·0672

Table 2. Differential cross sections (in units of 10^{-20} m^2 sr^{-1}) for electron scattering by potassium at 20 eV impact energy.

θ (deg)	Elastic	4^2P	5^2S+3^2D	5^2P	$4^2D+6^2S+4^2F+6^2P$	$5^2D+7^2S+5^2F$
5	—	499·0	51·5	5·70	4·42	1·92
10	24·9	63·8	13·1	2·91	1·97	0·870
15	9·94	15·4	5·04	1·39	1·05	0·487
20	3·40	2·72	1·70	0·490	0·817	0·327
30	1·58	0·503	0·616	0·0956	0·584	0·0647
40	1·49	0·192	0·173	0·00964	0·0859	0·0312
50	1·11	0·121	0·163	0·00544	0·0732	0·0139
60	0·446	0·0878	0·0669	0·0125	0·0223	0·0110
70	0·126	0·0748	0·0518	0·0117	0·0181	0·0101
80	0·0150	0·0210	0·0207	0·00270	0·00883	0·00462
90	0·0933	0·0374	0·0345	0·00457	0·0125	0·0104
100	0·219	0·0841	0·0482	0·0116	0·0158	0·0938
110	0·311	0·165	0·0716	0·0246	0·0308	0·0170
120	0·282	0·110	0·0621	0·0183	0·0243	0·0226

Table 3. Differential cross sections (in units of 10^{-20} m^2 sr^{-1}) for electron scattering by potassium at 40 eV impact energy.

θ (deg)	Elastic	4^2P	5^2S+3^2D	5^2P	$4^2D+6^2S+4^2F+6^2P$	$5^2D+7^2S+5^2F$
5	132·0	237·0	40·8	5·09	3·01	1·18
10	13·1	13·4	5·22	1·31	1·44	0·646
15	6·24	3·23	1·94	0·535	0·724	0·376
20	4·03	0·576	0·508	0·105	0·218	0·171
30	2·10	0·157	0·180	0·0129	0·0469	0·0239
40	1·38	0·0811	0·128	0·00826	0·0318	0·0164
50	0·768	0·0710	0·0722	0·00860	0·0207	0·0117
60	0·165	0·0299	0·0215	0·00342	0·00624	0·00408
70	0·0192	0·0128	0·0096	0·00151	0·00307	0·00209
80	0·0636	0·0136	0·0085	0·00080	0·00241	0·00166
90	0·156	0·0274	0·0107	0·00101	0·00233	0·00127
100	0·223	0·0424	0·0152	0·00316	0·00323	0·00195
110	0·239	0·0482	0·0143	0·00330	0·00416	0·00325
120	0·187	0·0396	0·0131	0·00318	0·00441	0·00243

uncertainties in the dimensions of the primary electron beam and the potassium target due to changes in the electron impact energy and the absolute crucible temperature, respectively. Variations in these parameters throughout a range which can reasonably be expected to encompass all the experimental conditions resulted in a change in the geometrical correction factor of 5%. The errors associated with the normalisation procedure are due to the errors in the optical oscillator strength (5%), the absolute energy scale (up to 13% at lower energies) and the 0·5° uncertainty in the angular position (a 3% error in the normalisation arises by shifting the angle scale by ±0·5° about the nominal 0° position).

For intermediate-energy electron scattering from potassium, data are available for elastic scattering as well as for the 4^2P and 5^2S+3^2D excitations. There are no previous data for the other transitions presented in our tables. For purposes of comparison we

Table 4. Differential cross sections (in units of 10^{-20} m^2 sr^{-1}) for electron scattering by potassium at 60 eV impact energy.

θ (deg)	Elastic	4^2P	5^2S+3^2D	5^2P	$4^2D+6^2S+4^2F+6^2P$	$5^2D+7^2S+5^2F$
5	66·5	139·0	22·7	3·70	2·68	0·640
10	12·9	4·58	2·84	0·776	1·08	0·518
15	7·16	0·988	0·924	0·228	0·441	0·181
20	3·33	0·226	0·244	0·0238	0·0856	0·0450
30	1·43	0·0694	0·112	0·00855	0·0293	0·0130
40	0·655	0·0291	0·0521	0·00422	0·0138	0·00654
50	0·261	0·0167	0·0203	0·00197	0·00608	0·00313
60	0·0518	0·00490	0·00673	0·00741	0·00252	0·00155
70	0·0115	0·00136	0·00272	0·00030	0·00099	0·00082
80	0·0539	0·00636	0·00331	0·00050	0·00008	0·00055
90	0·118	0·00172	0·00542	0·00146	0·00192	0·00126
100	0·156	0·0244	0·00755	0·00177	0·00209	0·00130
110	0·151	0·0240	0·00779	0·00180	0·00266	0·00163
120	0·112	0·0189	0·00669	0·00144	0·00182	0·00105

Table 5. Differential cross sections (in units of 10^{-20} m^2 sr^{-1}) for electron scattering by potassium at 100 eV impact energy.

θ (deg)	Elastic	4^2P	5^2S+3^2D	5^2P	$4^2D+6^2S+4^2F+6^2P$	$5^2D+7^2S+5^2F$
5	27·8	64·5	8·90	1·67	1·28	0·556
10	5·59	0·900	0·732	0·200	0·331	0·176
15	3·15	0·154	0·214	0·033	0·0923	0·0545
20	2·14	0·0772	0·107	0·0049	0·0272	0·0151
25	1·16	0·3098	0·0640	0·00370	0·0174	0·00714
30	0·656	0·0186	0·0378	0·00237	0·00938	0·00474
40	0·220	0·00532	0·0126	0·00038	0·00268	0·00177
50	0·0849	0·000551	0·00093	0·00036	0·00067	0·00042
60	0·0342	—	—	—	—	—
70	0·0342	—	—	—	—	—
80	0·0481	—	—	—	—	—
90	0·0611	—	—	—	—	—
100	0·0608	—	—	—	—	—
110	0·0447	—	—	—	—	—
120	0·0227	—	—	—	—	—

have chosen 7 and 60 eV electron impact energies. In figures 2, 3 and 4 are shown the elastic, 4^2P and 5^2S+3^2D cross sections respectively for 7 eV. Figures 5, 6 and 7 present DCS for the same transitions for 60 eV impact energy.

The experimental results of Williams and Trajmar (1977) at 6·7 eV, agree with the present measurements for the elastic scattering (figure 2) within the error limits of the two experiments for the angular range of 20 to 100°. It is to be noted, however, that the error limits on Williams and Trajmar's data are 50%. At angles below 20° and above 100° the differences in the two experimental results are rather large. The situation for the $4^2S \rightarrow 4^2P$ resonant transition cross section values (figure 3) is similar. In the preliminary measurements of Williams and Trajmar the temperature of the crucible was very high due to the use of electron-bombardment heating. This is evidenced by the

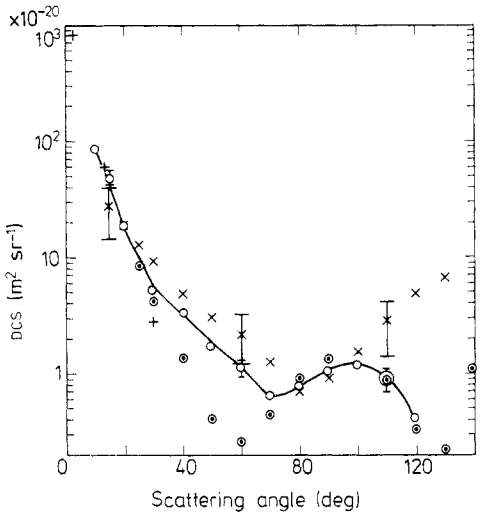

Figure 2. Elastic differential cross sections for 7 eV electron impact energy. ×, Williams and Trajmar (1977) (experimental $E_0 = 6{\cdot}7$ eV); +, Walters (1973, 1979, private communication) (theory); ⊙, Gehenn and Wilmers (1971) (experimental) and ○, present, joined by a visual fit full curve.

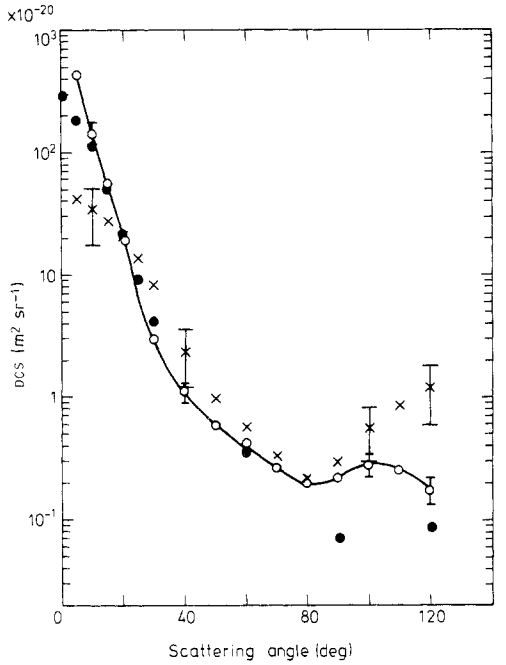

Figure 3. Differential cross sections for the resonance transitions $4^2S \rightarrow 4^2P$ obtained at 7 eV electron impact energy. ×, Williams and Trajmar (1977) (experimental $E_0 = 6{\cdot}7$ eV); ●, Kennedy *et al* (1977) (theory) and ○, present, joined by a visual fit full curve.

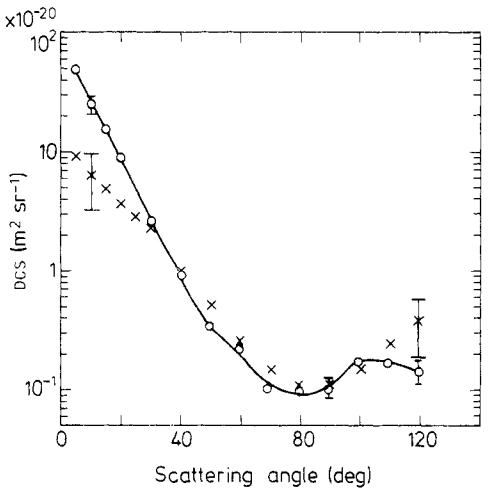

Figure 4. Differential cross sections for $4^2S \rightarrow 5^2S + 3^2D$ transitions obtained at 7 eV electron impact energy. ×, Williams and Trajmar (1977) (experimental) and ○, present, joined by a visual fit full curve.

fact that they observed double scattering (figure 1, Williams and Trajmar 1977) from the potassium beam which occurs for high beam densities generated by the higher crucible temperatures. At these temperatures the geometry of the potassium beam and electron beam can be distorted and may not remain the same as inferred from the initial

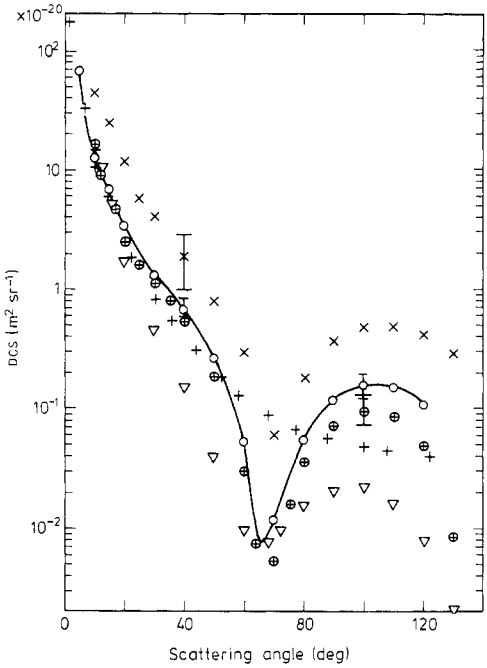

Figure 5. Elastic differential cross sections for 60 eV electron impact energy. ×, Williams and Trajmar (1977) (experimental); ⊕, Buckman *et al* (1979) (experimental); +, Walters (1973, 1979, private communication) (theory); ▽, Teubner *et al* (1978) (theory, $E_0 = 54{\cdot}4$ eV) and ○, present, joined by visual fit full curve.

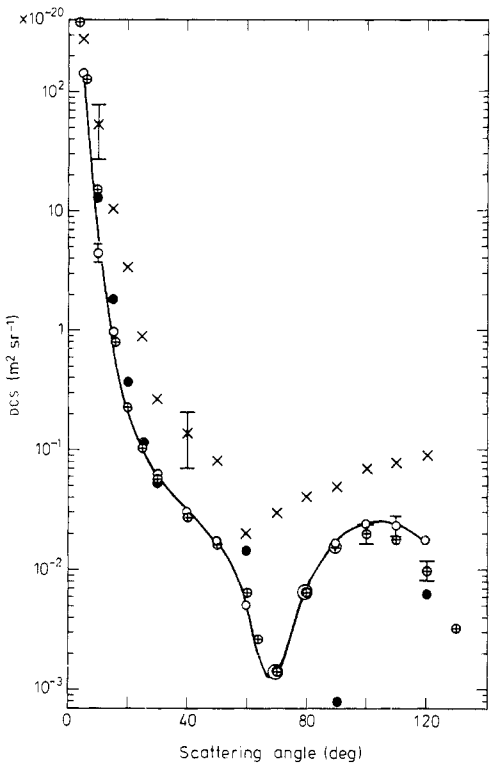

Figure 6. Differential cross sections for the resonance transitions $4^2S \rightarrow 4^2P$ obtained at 60 eV electron impact energy. ×, Williams and Trajmar (1977) (experimental); ⊕, Buckman *et al* (1979) (experimental); ●, Kennedy *et al* (1977) (theory) and ○, present, joined by a visual fit full curve.

alignment of the apparatus. Such geometrical distortions can cause gross errors in the angular distribution of the electron intensity especially at low and high scattering angles. We have performed the present experiment under lower and much better controlled temperature conditions. Moreover, as mentioned in § 2, the electron-bombardment heating used by Williams and Trajmar is not very suitable for low-temperature operation since small fluctuations in the temperature can cause large variations in the density of the atomic beam. These variations can contribute large errors in the scattered electron intensity. At 60 eV impact energy the shapes of the Williams and Trajmar curves for the 4^2P and $5^2S + 3^2D$ features are very similar to our own except at 70° where the present data have a minimum. However, the absolute values of Williams and Trajmar are about three times higher than the present data for these transitions. This discrepancy may be due to the fact that their method of normalisation of the measured relative values to the absolute scale is different than the one followed in the present work. Williams and Trajmar used the extrapolated total cross sections of Kasden *et al* (1973) (measured only up to 50 eV electron impact energy) to normalise their data. This value, as such, is higher by about a factor of two than the one obtained by us (figure 9). To this, one can add the error due to

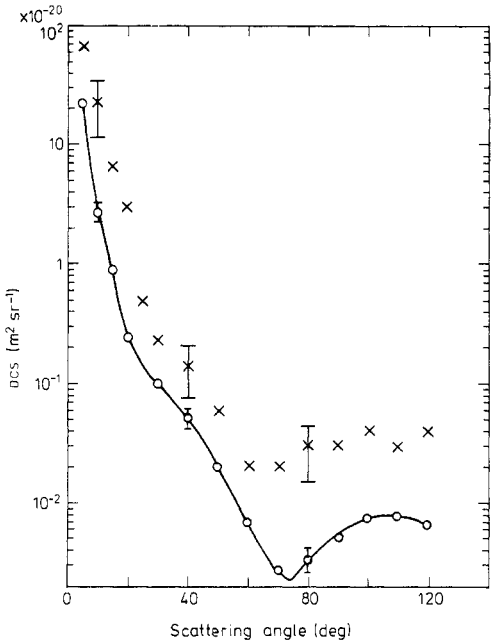

Figure 7. Differential cross sections for $4^2S \rightarrow 5^2S + 3^2D$ transitions obtained at 60 eV electron impact energy. ×, Williams and Trajmar (1977) (experimental) and ○, present, joined by a visual fit full curve.

extrapolating to zero-degree scattering angle which is very important at higher electron impact energies where the DCS curve for the resonant transition is very forward peaking. These combined effects can explain the differences between our values and those obtained by Williams and Trajmar (1977).

The experimental data of Gehenn and Wilmers (1971) for elastic scattering at 7 eV impact energy are in arbitrary units. We have normalised their data at 100° scattering angle to the present results. These data have a minimum around 60° which is not found in either the present work or that of Williams and Trajmar (1977). The remainder of their curve is in good agreement with the present data.

The experimental results of Buckman *et al* (1979) ($E_0 = 54{\cdot}4$ eV) for the elastic and resonant DCS are shown in figures 5 and 6 respectively. The elastic scattering cross section agrees quite well with the present data in the small angular region (up to 60° scattering angle). In the high angular region the difference is smaller than the combination of errors of the two measurements except for the DCS at 120°. At 100 eV impact energy the elastic scattering cross sections (not shown on the figures) agree even better with the present data at all scattering angles. The DCS for the resonance transition are in very good agreement at 54·4 eV (figure 6) and 100 eV (not shown on the figures) with the present data except for the largest measured angles.

The theoretical data of Walters (1973) and H R J Walters (1979, private communication) for elastic scattering and Kennedy *et al* (1977) for the resonance transitions $4^2S \rightarrow 4^2P$ are not available at the impact energies of our mesurements. By plotting their cross sections as a function of impact energy we have interpolated the theoretical DCS for the energies of our experiment. Both theoretical results agreed very well with the present data at small angles.

The optical-model calculation of Buckman *et al* (1979) for elastic scattering at 54·5 eV shows structure in the shape of the DCS with a minimum around 70° which is shallower than that of the present curve at 60 eV impact energy. However, there are large discrepancies in the absolute values except for the 12° and 16° points.

3.2. Integral and momentum transfer cross sections

In order to calculate integral and momentum transfer cross sections we need to know the DCS values between 0 and 5° (or 10°) and between 120 and 180°. Since most of the potassium transitions are very forward peaked, the small angular region DCS makes the major contribution, especially to the integral cross sections. For this reason we use different extrapolations for the different transitions; they will be explained later. Since in the present data the large-angle region does not contribute as much as the small-angle DCS, the extrapolation to 180° is not as critical. We use as a guide for the shape of the curves in the large-angular region the available theoretical or experimental results. The following definitions were employed to calculate the integral (σ_I) and momentum transfer (σ_M) cross sections:

$$\sigma_I = 2\pi \int_0^{\pi} \sigma(\theta) \sin\theta \, d\theta \tag{3}$$

and

$$\sigma_M = 2\pi \int_0^{\pi} \sigma(\theta) \sin\theta [1 - (k_f/k_i)\cos\theta] \, d\theta. \tag{4}$$

For the resonance transition $4^2S \rightarrow 4^2P$ we utilised the same procedure as explained in § 3.1 and were able to estimate the DCS for very small scattering angles. This procedure was also used to calculate the DCS in small angular steps in the region 0–10° for the purposes of better numerical integration. In this region, the DCS changes by five orders of magnitude at 100 eV and four orders of magnitude at 60 eV impact energy. As the impact energy is decreased this change is smaller, and at 7 eV it is only a factor of five.

Using equation (3) we calculate $\sigma_I(4^2P)$ and plot this result in figure 8 together with the results of Williams and Trajmar (1977) and Buckman *et al* (1979). The excitation measurements of Zapesochnyi *et al* (1976) and Chen and Gallagher (1978), as well as the theoretical results of Kennedy *et al* (1977) and Walters (1973) are also presented in this figure. Although the overall agreement with the results of Chen and Gallagher is good, the present results are lower by about 8·3, 3·3, 7·8, 6·0 and 8·6% for 7, 20, 40, 60 and 100 eV, respectively. Because of the small deviation (3·3 to 8·6%) from the measurements of Chen and Gallagher one can say that the normalisation procedure of the present measurements was satisfactory even for low incident energies (the present

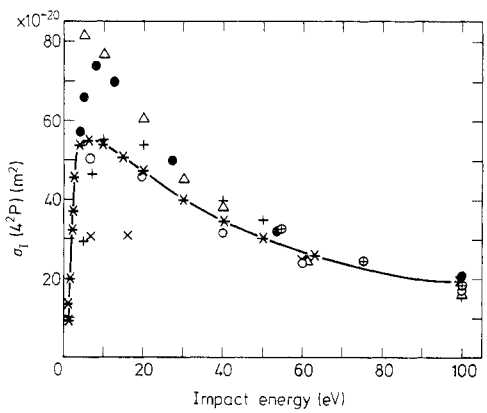

Figure 8. Integral excitation cross sections for resonance transitions $4^2S \rightarrow 4^2P$. ○, present; * Chen and Gallagher (1978) (experimental) joined by a visual fit full curve; ×, Williams and Trajmar (1977) (experimental); ⊕, Buckman *et al* (1979) (experimental); △, Zapesochnyi (1976) (experimental); +, Walters (1973) (theory) and ●, Kennedy *et al* (1977) (theory).

data are accurate within 20%). Agreement with other excitation measurements (Zapesochnyi *et al* 1976) is very good at 60 and 100 eV impact energy, but at low energies discrepancies are much higher than the error bars allowed by both sets of data. There is good agreement between all theortical and experimental results at higher incident energies.

The results of Williams and Trajmar are in good agreement with the present values of σ_I at 60 eV impact energy. This agreement is surprising because their DCS are about a factor of three higher than the present ones but can be understood in the light of very low-angle extrapolations. At lower impact energies their values of σ_I are about a factor of two lower than the present data. The results of Buckman *et al* (1979) are in reasonably good agreement for all energies.

Comparison with theoretical results shows that the present data agree much better with the Glauber calculations of Walters (1973) than with those of Kennedy *et al* (1977). Walter's data are within the error bars of the present results at all energies.

For other transitions the following procedure was used to estimate the small angular region DCS. For the third (5^2P) inelastic features in the energy-loss spectra (figure 1) we calculated the optical f values using the absolute DCS values at 5 and 10°. It is again assumed that $f_a^G(K)$ is a logarithmic function of K^2 as was done in the case of the resonance transition (4^2P) (§ 3.1). Once the optical f value has been calculated, the DCS in the region between 0 and 10° scattering angles can then be calculated from equation (1). For the second (5^2S+3^2D), fourth ($4^2D+6^2S+4^2F+6^2P$) and fifth ($5^2D+7^2S+5^2F$) inelastic features in the spectra we drew a straight line through the last two measured points to determine the zero-degree intercept on a semilogarithmic scale. This estimate was less critical since these curves contain many transitions and are less forward peaked at each impact energy. For elastic scattering we use the theoretical results of Walters' (1973) and H R J Walters (1979, private communication) in order to extrapolate the present curves to 0°.

Once all the transitions have been determined from 0–180° we calculate the integral (σ_I) and momentum transfer (σ_M) cross sections using relations (3) and (4). σ_I and σ_M are listed in tables 6 and 7, respectively. In our estimate the absolute value of σ_I and σ_M are accurate to 20%, except for the $4^2D+6^2S+4^2F+6^2P$ and $5^2D+7^2S+5^2F$ transitions for which the estimated error is about 40%. Errors are larger than those for the DCS because of additional errors in high angular region DCS evaluation.

Table 6. Integral, ionisation and total cross sections (in units of 10^{-20} m^2) for electron scattering by potassium.

	σ_I							
E_0 (eV)	Elastic	4^2P	5^2S+3^2D	5^2P	$4^2D+6^2S+4^2F+6^2P$	$5^2D+7^2S+5^2F$	σ_{ION}	σ_{TOT}
7	47·70	50·3	13·97	1·45	3·36	1·18	5·4†	123·0
20	17·60	45·9	6·79	1·14	1·45	0·58	8·4†	82·0
40	15·52	31·5	4·49	0·64	0·59	0·29	6·7‡	60·0
60	10·60	24·5	2·96	0·47	0·39	0·15	5·5‡	44·0
100	4·41	17·4	1·34	0·22	0·14	0·07	4·5‡	28·0

† Data from Korchevoi and Przonski (1967).
‡ Data from McFarland and Kinney (1965).

Table 7. Momentum-transfer cross sections (in units of 10^{-20} m^2) for electron scattering by potassium.

E_0 (eV)	Elastic	4^2P	5^2S+3^2D	5^2P	$4^2D+6^2S+4^2F+6^2P$	$5^2D+7^2S+5^2F$	σ_{MTOT}
7	10·48	9·50	4·78	0·73	1·42	0·88	27·8
20	4·03	3·20	1·19	0·302	0·44	0·28	9·4
40	3·12	1·15	0·41	0·065	0·09	0·05	4·9
60	2·37	0·52	0·18	0·036	0·047	0·024	3·2
100	0·61	0·19	0·10	0·025	0·014	0·012	1·0

Since we have obtained integral cross sections for the elastic and all the inelastic features below ionisation, we can obtain total cross sections, σ_{TOT}, from the following relation:

$$\sigma_{TOT} = \sigma_{EL} + \sigma_{INEL} + \sigma_{ION} \tag{5}$$

where σ_{EL} is the integral cross section for elastic scattering, σ_{INEL} the sum of integral cross sections for all inelastic features and σ_{ION} the cross section for ionisation. The values of σ_{TOT} in table 6 were derived using the ionisation (σ_{ION}) cross sections of Korchevoi and Przonski (1967) and McFarland and Kinney (1965). From this table it is apparent that the principal contribution to σ_{TOT} in potassium comes from σ_I of the resonance transitions $4^2S \rightarrow 4^2P$ especially at the higher energies. We assume that the inner-shell excitations are a negligible contribution to the total (σ_{TOT}) cross sections. In figure 9 are shown σ_{TOT} together with the theoretical data of Walters (1976) and the measured values of σ_{TOT} by Kasden *et al* (1973). The present data are in excellent agreement with the calculation of Walters. The shape of the present curve is different from that of Kasden *et al*, but the absolute values of Kasden *et al* are within the error bars of the present data except at 50 eV impact energy.

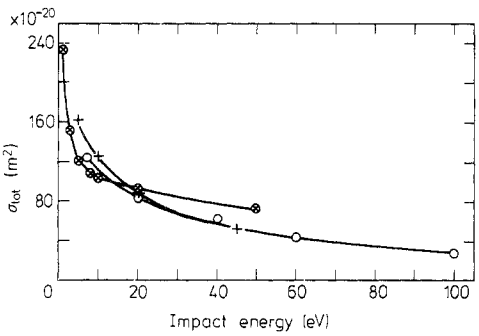

Figure 9. Total cross sections. ○, present; +, Walters (1976) (theory) and ⊗, Kasden *et al* (1973) (experimental). All are joined by a visual fit full curve.

The momentum transfer cross sections, σ_M, connected with the elastic scattering and the various transitions are presented in table 7. Williams and Trajmar (1977) have also obtained σ_M values for the elastic and the first two inelastic features (figure 1). They are not shown in table 7. However, it is found that the present results are two to three times lower than their results except at 7 eV impact energy where the σ_M for elastic scattering are lower by a factor of five. This may be due to their higher DCS values at angles of 100° and above, which have already been discussed in § 3.1. We have used

the sum σ_M (elastic) + σ_M (inelastic) to obtain the total momentum transfer cross section $\sigma_{M_{TOT}}$ which does not include the cross sections connected with ionisation. They are also presented in table 7 where it is seen that the largest contribution comes from elastic scattering.

Acknowledgments

The authors wish to express their appreciation to Dr S Trajmar for valuable discussions. The authors owe special gratitude to Dr D F Register for extended discussions on the subject and for help in data processing. The authors also acknowledge the help of Mr G R Steffensen in computer programming.

References

Bethe H A 1930 *Ann. Phys., Lpz* **5** 325–400
Bransden B H and McDowell M R C 1978 *Phys. Rep.* **46** 249–394
Brinkmann R and Trajmar S 1980 *J. Phys. E: Sci. Instrum.* **11** 894
Buckman S J, Noble C J and Teubner P J O 1979 *J. Phys. B: Atom. Molec. Phys.* **12** 3077–91
Chen S T and Gallagher A C 1978 *Phys. Rev.* A **17** 551–60
Dalgarno A and Davison W D 1967 *Molec. Phys.* **13** 479–86
Dillon M and Lassettre E N 1975 *J. Chem. Phys.* **62** 2373–90
Fink M and Yates A C 1970 *Atomic Data* **1** 385–97
Gehenn W and Wilmers M 1971 *Z. Phys.* **244** 395–401
Inokuti M 1971 *Rev. Mod. Phys.* **43** 297–347
Kasden A, Miller T M and Bederson B 1973 *Phys. Rev.* A **8** 1562–9
Kennedy J V, Myerscough V P and McDowell M R C 1977 *J. Phys. B: Atom. Molec. Phys.* **10** 3759–80
Korchevoi Yu P and Przonski A M 1967 *Sov. Phys.-JETP* **24** 1089–92
Lassettre E N 1965 *J. Chem. Phys.* **43** 4479–86
Lassettre E N and Dillon M A 1973 *J. Chem. Phys.* **59** 4778–83
Lassettre E N and Skerbele A 1974 *J. Chem. Phys.* **60** 2464–9
Lasettre E N, Skerbele A and Dillon M A 1969 *J. Chem. Phys.* **50** 1829–39
—— *J. Chem. Phys.* **52** 2797–9
McFarland R H and Kinney J D 1965 *Phys. Rev.* A **137** 1058–61
McMillan J H 1934 *Phys. Rev.* **46** 983–8
Moiseiwitsch B L and Smith S J 1968 *Rev. Mod. Phys.* **40** 238–353
Skerbele A and Lassettre E N 1973 *J. Chem. Phys.* **58** 2887–92
Trajmar S, Williams W and Srivastava S K 1977 *J. Phys. B: Atom. Molec. Phys.* **10** 3323–33
Vogt R E, Cook W R, Cummings A C, Garrard T L, Gehrels N, Stone E C, Trainor J H, Schardt A W, Conlon T, Lal N and McDonald F B 1979 *Science* **204** 1003–6
Vušković L, Trajmar S and Register D 1981 *Phys. Rev.* A to be published
Walters H R J 1973 *J. Phys. B: Atom. Molec. Phys.* **6** 1003–19
—— 1976 *J. Phys. B: Atom. Molec. Phys.* **9** 227–37
Williams W and Trajmar S 1977 *J. Phys. B: Atom. Molec. Phys.* **10** 1955–66
Zapesochnyi I P, Postoi E N and Aleksakhin I S 1976 *Sov. Phys.-JETP* **41** 865–70